

Improvement of Texture and Magnetic Properties in 4.5 wt.% Si Grain-Oriented Electrical Steels

JinLong Liu^{a*}, Han Zhang^a, Ning Shan^a, YuHui Sha^a, Fang Zhang^a, Liang Zuo^a

^aKey Laboratory for Anisotropy and Texture of Materials (Ministry of Education), School of Materials Science and Engineering, Northeastern University, Shenyang, China

Received: November 25, 2018; Revised: June 16, 2019; Accepted: July 02, 2019

4.5 wt.% Si grain-oriented electrical steel sheets were successfully produced by hot rolling, normalizing, warm rolling and annealing, and texture evolution was investigated using macro- and micro-texture analysis. It is found that the recrystallization texture of sheets is very sensitive to the warm rolling reduction, and 83-87% warm rolling reductions are more favorable to η texture ($\langle 100 \rangle // \text{RD}$, rolling direction) evolution during secondary recrystallization, and consequently the magnetic induction B_8 is significantly improved to 1.69-1.70 T in this rolling reduction range. The decreased B_8 in the 89% warm rolled sheet is ascribed to the obviously decreased primary recrystallization η fiber, which leads to the insufficient quantity of η grains in the early stage of abnormal grain growth. The results obtained in the current work can provide an efficient way to improve the recrystallization texture of 4.5 wt.% Si grain-oriented electrical steel sheets.

Keywords: grain-oriented, electrical steels, texture, secondary recrystallization.

1. Introduction

Grain-oriented electrical steels with silicon content less than 3.5 wt.%, which have ultrahigh permeability and low core loss, are widely used as core materials in transformers of power and electronic industries. Increasing silicon content to 4.5 wt.% can effectively reduce the iron loss of grain-oriented electrical steels, especially at high frequency. The magnetic property of 4.5 wt.% Si grain-oriented electrical steels is highly sensitive to the recrystallization texture, which is still far from efficient optimization.

The reduction ratio of warm rolling and cold rolling is an important factor to influence the microstructure and texture evolution during deformation and recrystallization, and further affects the magnetic properties in grain-oriented electrical steels. The average grain size of primary recrystallization decreases as the increase of the reduction ratio and will be constant when the reduction ratio is large enough^{1,2}. Moreover, both the intensity and the type of primary recrystallization texture can be modified by controlling the strain stored energy of grains and the preferred nucleation sites including grain boundaries, deformation bands, shear bands, which are also closely related to the reduction ratio. Samajdar³ found that there are two kinds of shear bands in the cold rolled sheets of 3.0 wt.% Si grain-oriented silicon steels. Shear bands inclined at 37° with the rolling direction (RD) are usually formed at 25-77% reductions³⁻⁵, while those inclined at 20° with RD can remain at 85-90% reductions. Among them, accurate Goss ($\{110\} \langle 001 \rangle$) orientation prefers to nucleate

at 20° shear bands³. If the reduction ratio increases to above 90%, the magnetic induction will decrease rapidly due to the lack of secondary Goss nuclei and the increase of grains with other orientation, which have a competitive relationship with Goss grains during abnormal growth process⁶.

In current work, the 4.5 wt.% Si grain-oriented electrical steel sheets were produced by hot rolling, warm rolling, primary recrystallization and secondary recrystallization annealing. The development of texture and microstructure in the sheets under different reduction ratios were analyzed to explore the improving methods of texture and magnetic properties in 4.5 wt.% Si grain-oriented electrical steels.

2. Experiments

Fe-4.5 wt.% Si ingots were prepared by vacuum induction melting, and the chemical composition is shown in Table 1. The ingots were first homogenized at 1250 °C and forged to 40 mm, and then hot rolled to 1.8 mm. Next, hot bands were normalized at 1020 °C for 7 min and further warm rolled to 0.30, 0.24 and 0.20 mm at 200 °C with total reductions of 83, 87 and 89%, respectively. Afterwards, primary recrystallization annealings of warm rolled sheets, including decarburization and nitriding annealing, were conducted in a tube furnace. During the decarburization treatment, the warm rolled sheets were annealed at 830 °C for 5 min in a wet N₂ atmosphere. The specimens were heated up to 780 °C and soaked for 0.5 min in a NH₃ atmosphere for nitriding. Finally, secondary

*e-mail: liujl@atm.neu.edu.cn.

recrystallization annealing was carried out in a mixed N_2 - H_2 atmosphere with a heating rate of 20 °C/h up to 1200 °C and then the sheet was annealed at 1200 °C for 5 h under a 100% H_2 atmosphere for purification.

Table 1. Chemical composition of the material (Weight percent).

Si	C	Mn	Al	S	Ni	Fe
4.5	0.03	0.1	0.05	0.02	0.3	Bal.

The pole figures of rolled and annealed sheets were measured at one-quarter thickness layer by X-ray diffraction. And the orientation distribution functions (ODFs) were calculated from pole figures. Here, the one-quarter thickness layer is defined by the equation $a/d = 1/4$, where a represents the distance away from the surface layer and d is the whole sheet thickness. Electron backscattered diffraction (EBSD) analysis was also performed to investigate the recrystallization texture. Optical microscopy and EBSD were applied on longitudinal sections as defined by the rolling direction (RD) and the normal direction (ND). Moreover, the magnetic flux density at a field strength of 800 A/m (B_8) and iron loss at 1.5 T and 50 Hz ($P_{15/50}$) were measured by using a single sheet tester along RD.

3. Results and Discussion

3.1 Microstructure and texture after hot rolling and warm rolling

The hot rolling microstructure is mainly composed of elongated grains through thickness (Figure 1), which is different from the heterogeneous microstructure of hot bands in 3.0 wt.% Si grain-oriented silicon steels with fine grains at the surface, coarse grains in the intermediate layer, and elongated grains in the center according to the report of Li⁷. This relatively homogeneous microstructure in Fe-4.5 wt.% Si hot bands can be ascribed to the vanished austenite due to the high Si content and relatively low carbon content of 0.03 wt.% in the present study. It can be known from the phase diagram of Fe-Si-C reported by Tsai⁸ that austenite deformation is difficult to be involved in the whole hot rolling process in Fe-4.5 wt.% Si-0.03 wt.% C silicon steels. Akta⁹ reported that dynamic recovery rate of ferrite in steels is about two orders of magnitude higher than that of austenite. Therefore, recrystallization is difficult to occur during hot rolling after sufficient dynamic recovery in this steel and the dynamic recovery microstructure forms through the hot band thickness as presented in Figure 1(a). The main texture component of hot bands is Goss (Figure 1(b)), which is similar to the 3.0 wt.% Si silicon steels¹⁰. After normalizing annealing, the hot band is completely recrystallized and the intensity of Goss clearly weakens.

The warm rolling texture of Fe-4.5 wt.% Si thin sheet under 83% reduction is mainly composed of α ($\langle 110 \rangle // RD$) and γ ($\langle 111 \rangle // ND$) fibers. And the warm rolling microstructure in the longitudinal section is characterized by elongated grains with some in-grain shear bands, as shown in Figure 2. Figure 3 further shows the orientation densities along α and γ fibers of warm rolled sheets under various reductions. It is found that warm rolling sheets under 83% and 87% reduction have the similar texture type, which is mainly composed of strong α fiber peaked at $\{001\} \langle 110 \rangle$ and strong γ fiber peaked at $\{111\} \langle 110 \rangle$. As the reduction increases to 89% (Figure 3), orientation densities along α fiber, especially $\{112\} \langle 110 \rangle$ component, sharply increase, and the γ fiber also enhances. Compared with $\{111\} \langle 112 \rangle$ and $\{111\} \langle 110 \rangle$ grains, $\{112\} \langle 110 \rangle$ grains have smaller Taylor factor¹¹, which is not conducive to the formation of shear bands. It is known that the η grains ($\langle 100 \rangle // RD$) mainly nucleated at the shear bands^{3,12} in silicon steels. Therefore, the condition of 89% reduction is not beneficial to the nucleation of η grains in the early stage of primary recrystallization.

3.2 Microstructure and texture of primary and secondary recrystallization

After decarburization annealing at 830 °C, warm rolled Fe-4.5 wt.% Si sheets under different reductions are completely recrystallized. For the sheet under 83% reduction, the microstructure consists of uniform equiaxed grains with the average grain size of 16 μm , and the primary recrystallization texture mainly consists of γ fiber with peak at $\{111\} \langle 112 \rangle$ as well as comparatively weak η fiber and λ ($\langle 001 \rangle // ND$) fiber (Figure 4). When the warm rolling reduction increases to 87-89%, the grain size after decarburization annealing at 830 °C decreases to about 13 μm . Moreover, the orientation densities along main texture fibers exhibit an evident dependence on warm rolling reduction, as shown in Figure 5. At 83 and 87% reductions, γ fiber is dominant, and there also exists weak λ and η fibers. As warm rolling reduction increases to 89%, γ fiber still dominates the primary recrystallization texture, and λ fiber nearly keeps unchanged, while η fiber decreases significantly.

Figure 6 shows the orientation image maps and micro-texture of the sample after warm rolling with 83% reduction and annealing at 830 °C for 5 min. The micro-texture is characterized with relatively strong γ and λ fibers and weak η fiber, which is obviously different from the macro-texture in Figure 4(b). The difference between the micro-texture and macro-texture can be attributed to the texture gradient through the sheet thickness. The micro-texture is observed on longitudinal sections that contain the center layer with strong plane strain, while the macro-texture is measured at quarter layer. The center layer usually has stronger λ fiber after primary recrystallization in silicon steels¹³. Figure 6(c) further gives the number fractions of main texture fibers in

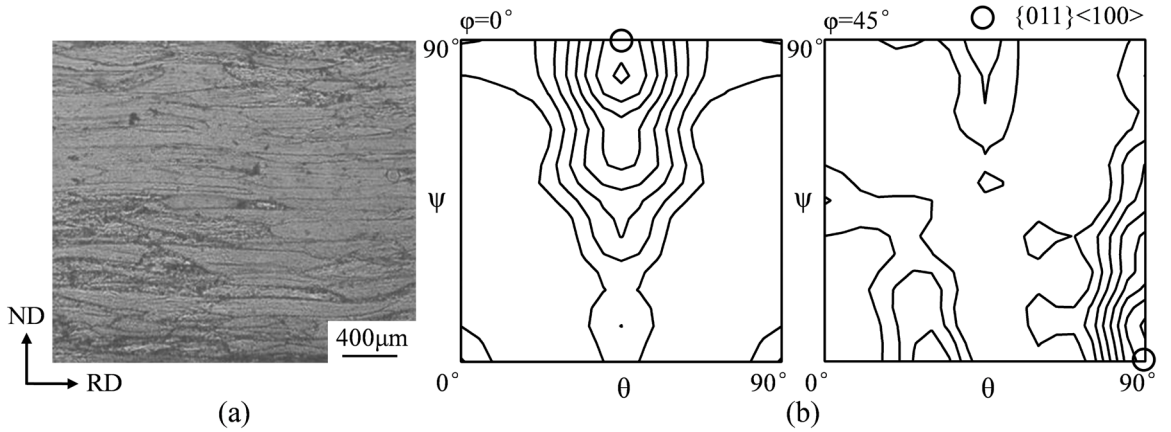


Figure 1. (a) Microstructure and (b) constant $\phi = 0^\circ$ and 45° sections of ODFs (levels: 1, 2, 3...) of Fe-4.5 wt.% Si hot bands.

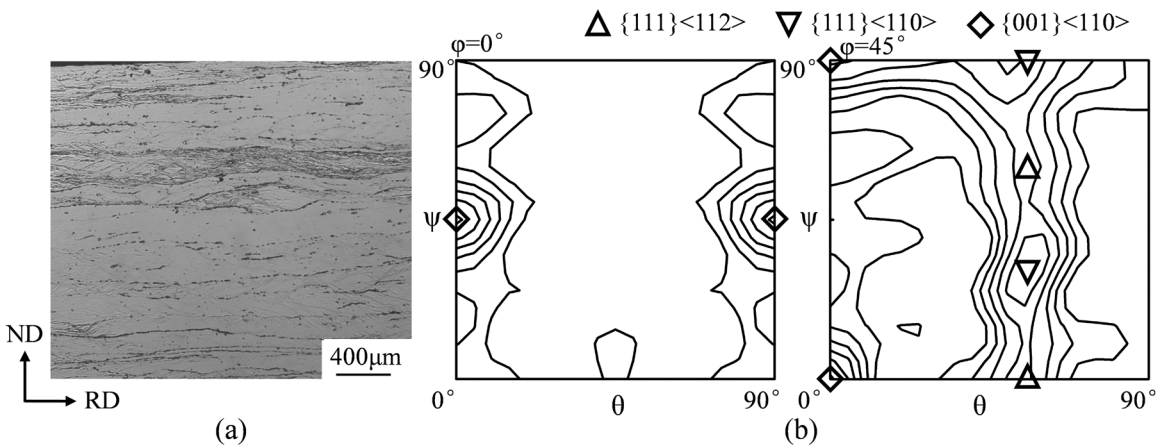


Figure 2. (a) Microstructure and (b) constant $\phi = 0^\circ$ and 45° sections of ODFs (levels: 1, 2, 3...) of warm rolled Fe-4.5 wt.% Si sheets under 83% reduction.

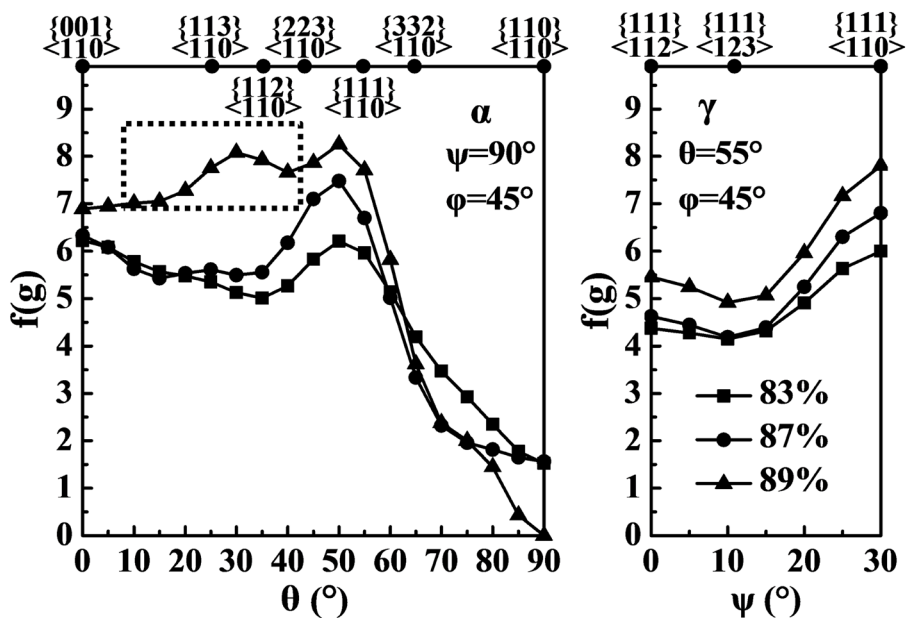


Figure 3. Orientation densities along α and γ fibers of warm rolled Fe-4.5 wt.% Si sheets under different reductions.

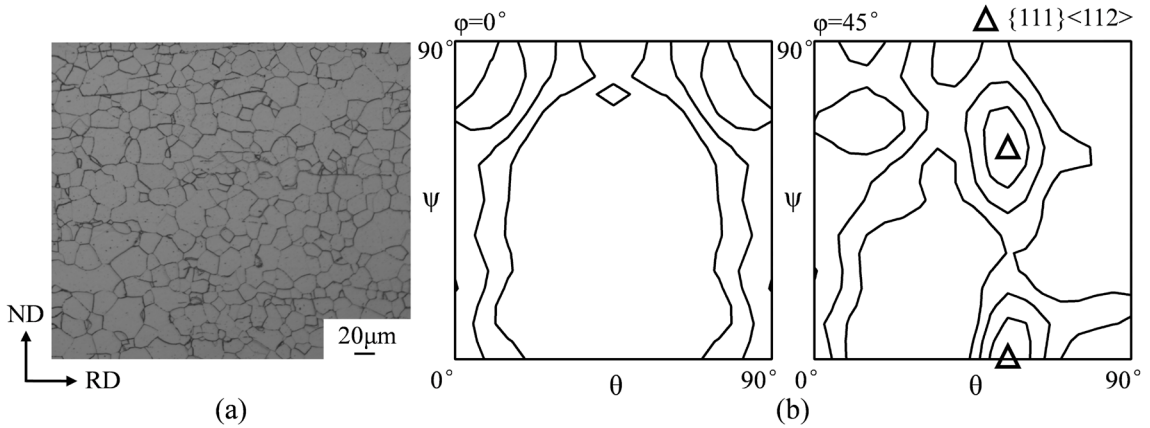


Figure 4. (a) Microstructure and (b) constant $\phi = 0^\circ$ and 45° sections of ODFs (levels: 1, 2, 3...) in Fe-4.5 wt.% Si sheets after decarburization annealing at 830°C for 83% reduction.

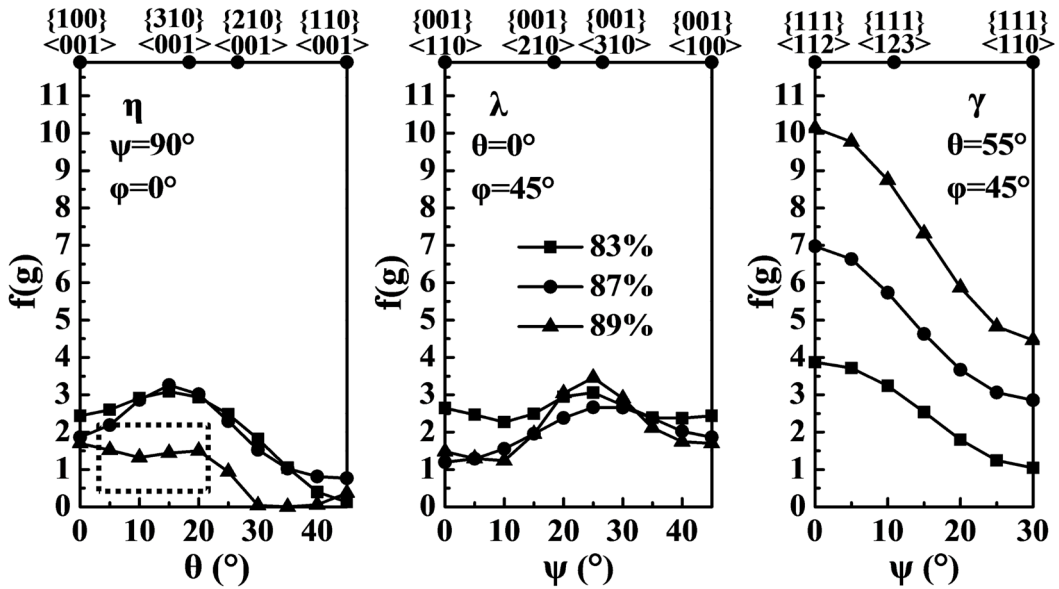


Figure 5. Orientation densities along η , λ and γ fibers in Fe-4.5 wt.% Si sheets after decarburization annealing at 830°C for different reductions.

various grain size ranges. It can be found that the fractions of η and λ increase sharply beyond the grain size of $25\ \mu\text{m}$, while γ has a much higher fraction in the range of $5\text{-}20\ \mu\text{m}$. This demonstrates distinctly that a large number of relatively fine γ grains exist in the sheets after decarburization annealing in current work, although the intensity of γ fiber is clearly weaker than that investigated by Hölscher¹⁴. It is generally believed that the formation of a large number of fine primary recrystallized γ grains, especially $\{111\}\langle 112\rangle$ grains, is beneficial to the secondary recrystallization of η grains in grain-oriented silicon steels because of the high migration rate of the grain boundary between them¹⁵.

The micro-texture of the sample after warm rolling with 89% reduction and annealing at 830°C for 5 min

is mainly composed of strong γ fiber, weak λ fiber, and weak η fiber, as shown in Figure 7, which is completely different from the micro-texture in Figure 6. From the micro-texture characteristics in Figures 6 and 7, it can be seen that with the increase of warm rolling reduction from 83% to 89%, the γ fiber increases sharply and η fiber decreases, which is consistent with the macro-texture results of Figures 4 and 5.

After purification annealing at 1200°C , all Fe-4.5 wt.% Si sheets under different reductions are completely secondary recrystallized. The microstructure and texture of sheets under 83% and 89% reductions are shown in Figures 8 and 9, respectively. The huge grains more than 1 mm develop and the texture is composed of strong η fiber with peak at

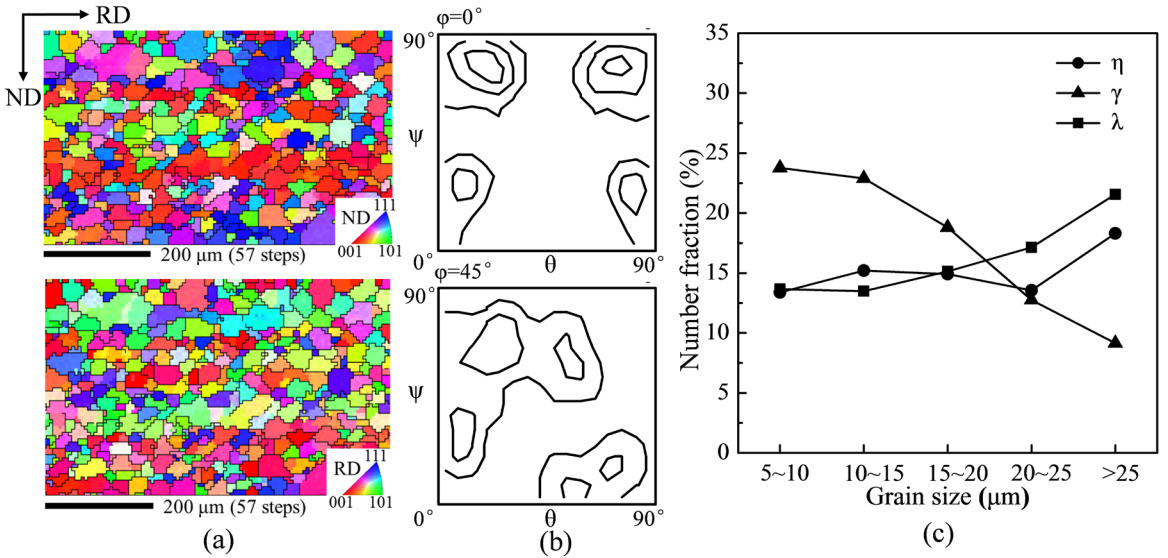


Figure 6. (a) Orientation image maps, (b) constant $\phi = 0^\circ$ and 45° sections of ODFs (levels: 1, 2, 3...) and (c) number fraction distribution of main texture components in different size ranges in Fe-4.5 wt.% Si sheets after decarburization annealing at 830°C for 83% reduction.

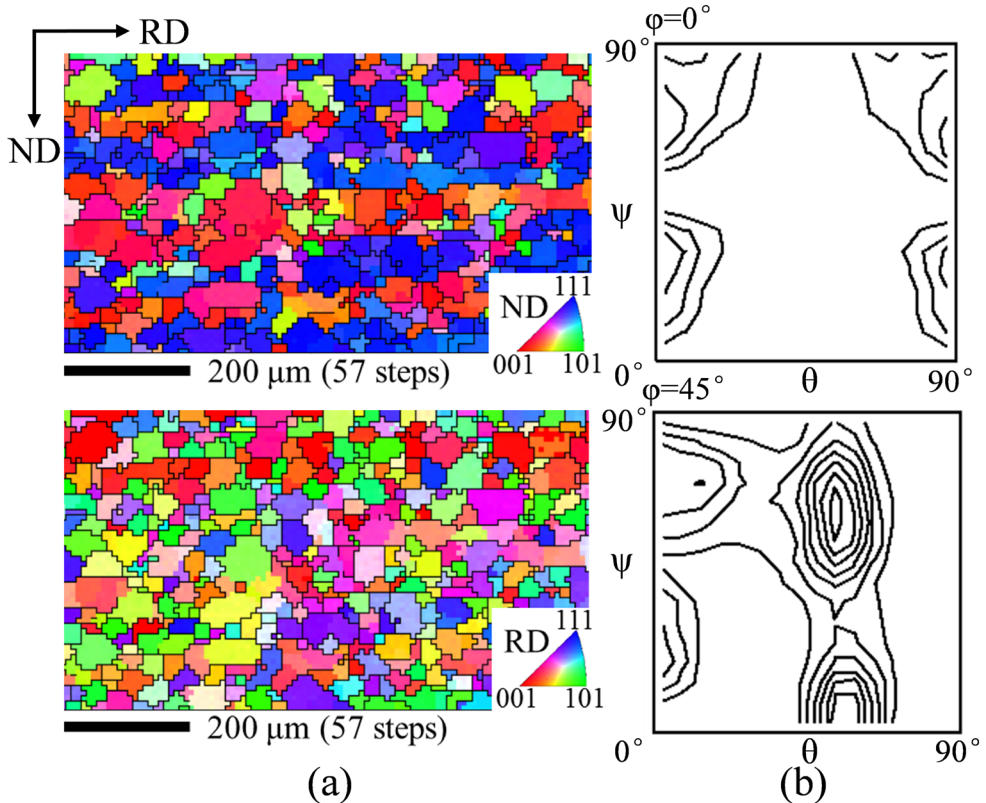


Figure 7. (a) Orientation image maps and (b) constant $\phi = 0^\circ$ and 45° sections of ODFs (levels: 1, 2, 3...) in Fe-4.5 wt.% Si sheets after decarburization annealing at 830°C for 89% reduction.

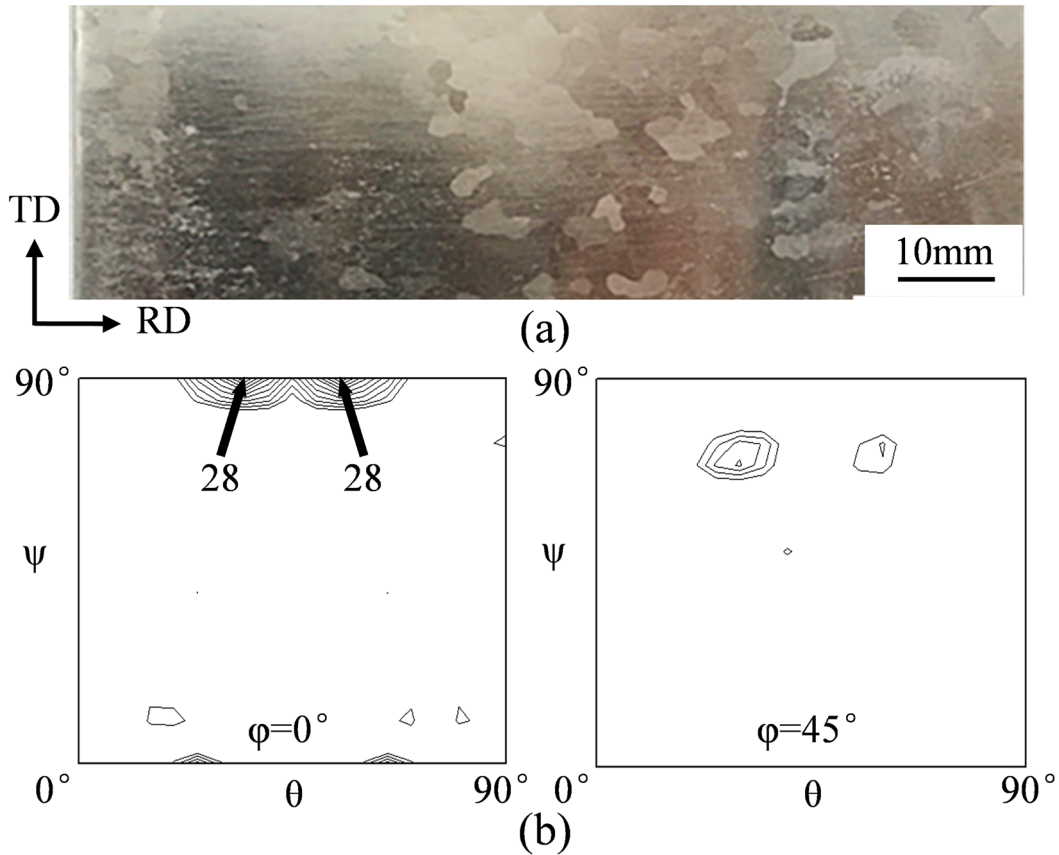


Figure 8. (a) Microstructure and (b) constant $\phi = 0^\circ$ and 45° sections of ODFs (levels: 8, 10, 12...) of 83% warm rolled Fe-4.5 wt.% Si sheets after purification annealing at 1200°C .

$\{320\}\langle 001\rangle$ for both sheets. And the $\{320\}\langle 001\rangle$ weakens with the increase of reduction ratio.

It should be noted that the abnormal growth grains in the present work were not the Goss grains, which are different from the results in most of 3.0 wt.% Si grain-oriented silicon steels^{3,15}. The microstructure and the constant $\phi = 0^\circ$ and 45° sections of ODFs in Figures 8 and 9 show that the $\{320\}\langle 001\rangle$ grains abnormally grow rather than Goss grains. Lu¹⁶ prepared a 0.23 mm grain-oriented 4.5 wt.% Si steel sheet by strip casting, hot rolling, one-stage warm rolling, primary annealing, and secondary annealing. It was found that a strong Goss texture develops after secondary annealing. Therefore, the $\{320\}\langle 001\rangle$ secondary recrystallization texture is not a special result in 4.5 wt.% Si grain-oriented silicon steels. Moreover, Zhang¹⁷ also reported that the abnormal growth of η grains in silicon steels except for the Goss grains, but did not explain the formation mechanism. It is known that both $\{320\}\langle 001\rangle$ and Goss texture have the same easy magnetization direction $\langle 001\rangle$ along the rolling direction, which meets the texture control requirements of grain-oriented silicon steels. However, the mechanism^{15,18} of secondary recrystallization of grain-oriented silicon steel shows that the special angle between Goss and $\{111\}\langle 112\rangle$

grains is an important key for the rapid migration of Goss grain boundaries at the initial stage of secondary recrystallization. If the selectively growing grains are not Goss grains, this special angle no longer exists. Therefore, the selective growth mechanism of $\{320\}\langle 001\rangle$ grains is an interesting issue in further investigation.

The magnetic inductions (B_8) of all recrystallized sheets along RD achieve 1.59-1.70 T and the iron losses ($P_{15/50}$) are between 1.63-1.78 W/kg, as shown in Figure 10. The sheets under the 83 and 87% reductions have the similar magnetic induction of about 1.70 T, which are close to the 1.73 T measured in a 4.5 wt.% Si grain-oriented steels produced by the special strip casting method¹⁶. It should be noted that the magnetic induction significantly drops to 1.59 T for the 89% reduction, although considerable number of η grains occur complete secondary recrystallization. In addition, the iron loss in Figure 10(b) is high compared with other reports¹⁵, because the iron loss is sensitive to many factors such as the grain size, the quality of sheets surface and magnetic domain size, etc. And the main issues discussed in this paper is about the optimizing texture and magnetic induction of 4.5 wt.% Si grain-oriented steels by controlling the warm rolling reductions.

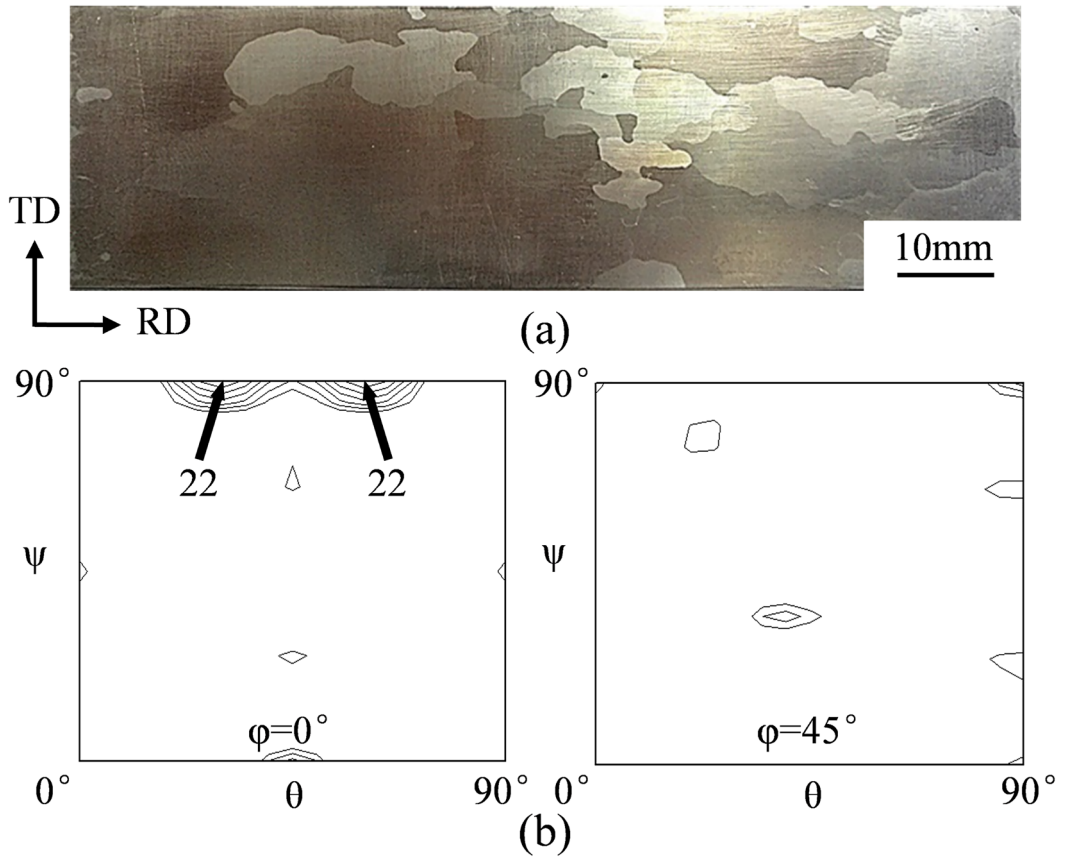


Figure 9. (a) Microstructure and (b) constant $\phi = 0^\circ$ and 45° sections of ODFs (levels: 8, 10, 12...) of 89% warm rolled Fe-4.5 wt.% Si sheets after purification annealing at 1200 °C.

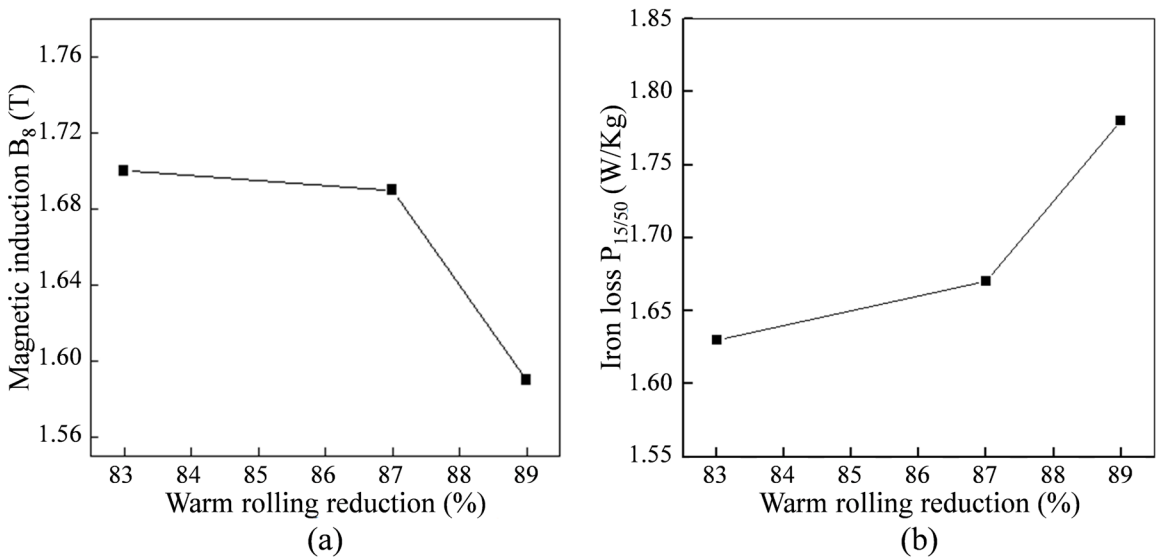


Figure 10. (a) Magnetic induction and (b) iron loss in Fe-4.5 wt.% Si sheets after purification annealing at 1200 °C.

3.3 Effect of warm rolling reduction on the texture and magnetic properties

In present study, strong secondary recrystallization η texture is developed and the magnetic induction B_8 achieves 1.69-1.70 T in 4.5 wt.% Si grain-oriented silicon steels produced by the common rolling and annealing method in the case of 83-87% warm rolling reductions. Moreover, the slightly increased reduction to 89% significantly results in the sharp deterioration of magnetic induction. Therefore, the discussion will focus on the relation between warm rolling reduction and the formation of strong η texture in 4.5 wt.% Si grain-oriented silicon steels.

The high magnetic susceptibility of grain-oriented silicon steel is mainly derived from strong and sharp η texture, and accurate η grains usually nucleate at shear bands inclined by 20° to RD³, which approach the number peak at an extremely narrow range of 87-88%^{19,20} reductions in 3.0 wt.% Si grain-oriented silicon steels, while the proper range is extended to 83-87% in 4.5 wt.% Si grain-oriented silicon steels according to the magnetic properties in Figure 10. The lower limit of suitable warm rolling reduction is reduced to 83%, which is reasonably related with the heterogeneous deformed microstructure. It is known that the characteristic of shear bands is closely related with the deformation behaviour such as activation of slip systems and work hardening²¹. The strong deformation γ fiber can promote the formation of shear bands due to the prominent orientation softening once localized shear occurs²². The increase of the tendency of strength with adding Si content in grain-oriented silicon steels acts as an additional factor, since the solution strengthening can also promote the progress of localized shear. In addition, the shear bands which provides the nucleation sites of η grains are mainly formed in the γ deformed grains of grain-oriented silicon steels^{3,12}. In γ deformed grains, severe strain localization is necessary for the initiation of shear bands²³ and the high ductility is required to ensure the formation of both strong γ rolling texture. However, the brittleness of 4.5 wt.% Si grain-oriented silicon steels at room temperature hinders the formation of γ rolling texture. Therefore, the significantly improved ductility of 4.5 wt.% Si grain-oriented silicon steel sheets under warm rolling conditions provides adequate deformation for the initiation and development of shear bands in γ grains.

When the rolling reduction reaches up to 89%, the α fiber especially $\{112\}\langle 110\rangle$ component clearly enhances (Figure 3). Based on the report¹¹, $\{112\}\langle 110\rangle$ component has a relatively small Taylor factor, which seriously hinders the localized accumulation of dislocation slip resistance and the onset of shear bands. Thus the intensity of primary recrystallization η fiber for 89% warm rolling reduction obviously decreases (Figure 5).

During the process of secondary recrystallization, abundant η grains can abnormally grow in the 83-87% warm rolled sheets. In contrast, grains with various orientations may preferentially grow during high temperature annealing in the 89% warm rolled sheets due to the insufficiency of η grains in primary recrystallization stage (Figure 5). Therefore, the decreased B_8 in the 89% warm rolled sheet can be ascribed to the obvious decline of primary recrystallization η fiber, which further leads to the insufficient quantity of η grains during the process of abnormal grain growth.

3.4 Effects of processing parameters on the secondary recrystallization of η grains

In current work, the designed chemical composition and the applied parameters of hot rolling, normalizing, cold rolling and annealing processes are responsible for the development of strong η texture and thus for the achievement of 1.70 T magnetic induction B_8 . Firstly, a large reduction of 95.5% was adopted during hot rolling to enhance the Goss texture as the ideal initial texture. Secondly, carbon content, hot rolling and normalizing annealing are appropriate to ensure the formation of relatively homogeneous equiaxed grains in the different layers of normalizing hot bands. Thirdly, the rolling reductions of 83-87% accompanied with temperature of 200 °C are beneficial to modify the orientation and density of shear bands. Finally, the slow heating rate of 20 °C/h is favorable to the incubation and accumulation of size advantage of secondary recrystallization η grains. This experiment shows the possibility of producing 4.5 wt.% Si grain-oriented silicon steels by the one-stage cold rolling method in the common industrial lines of producing grain-oriented silicon steels.

4. Conclusions

By designing the chemical composition and fabricating parameters including hot rolling, normalizing, warm rolling and annealing, the strong η texture was successfully developed in 4.5 wt.% Si grain-oriented silicon steel sheets after secondary recrystallization. The magnetic property is evidently depended on the warm rolling reduction. The high magnetic induction B_8 of 1.69-1.70 T is achieved at 83 and 87% reductions, while B_8 is only 1.59 T at 89% reduction, although considerable number of η grains occur complete secondary recrystallization. The decreased B_8 in the 89% warm rolled sheet can be ascribed to the obvious decline of primary recrystallization η fiber, which further leads to the insufficient quantity of η grains during the process of abnormal grain growth.

5. Acknowledgements

This work was supported by the National Key Research and Development Program of China (No. 2016YFB0300305);

National Natural Science Foundation of China (No. 51671049); Fundamental Research Funds for the Central Universities (No. N170213019); and China Scholarship Council (CSC) (No. 201806085006).

6. References

1. Dorner D, Zaefferer S, Lahn L, Raabe D. Overview of Microstructure And Microtexture Development in Grain-oriented Silicon Steel. *Journal of Magnetism and Magnetic Materials*. 2006;304(2):183-186.
2. Taguchi S, Sakakura A. The effects of AlN on secondary recrystallization textures in cold rolled and annealed (001) [100] single crystals of 3% silicon iron. *Acta Metallurgica*. 1966;14(3):405-423.
3. Samajdar I, Cicale S, Verlinden B, Van Houtte P, Abbruzzese G. Primary recrystallization in a grain oriented silicon steel: on the origin of goss {110}<001> grains. *Scripta Materialia*. 1998;39(8):1083-1088.
4. Liu JL, Sha YH, Zhang F, Li JC, Yao YC, Zuo L. Development of {210} <001> recrystallization texture in Fe-6.5 wt.% Si thin sheets. *Scripta Materialia*. 2011;65(4):292-295.
5. Cicalè S, Samajdar I, Verlinden B, Abbruzzese G, Houtte PV. Development Of Cold Rolled Texture and Microstructure in a Hot Band Fe-3%Si Steel. *ISIJ International*. 2002;42(7):770-778.
6. Kim JK, Woo JS, Chang SK. Influence of annealing before cold rolling on the evolution of sharp Goss texture in Fe-3%Si alloy. *Journal of Magnetism and Magnetic Materials*. 2000;215-216:162-164.
7. Li Y, Mao WM, Yang P. Inhomogeneous Distribution of Second Phase Particles in Grain Oriented Electrical Steels. *Journal of Materials Science & Technology*. 2011;27(12):1120-1124.
8. Tsai MC, Hwang YS. The quenching effects of hot band annealing on grain-oriented electrical steel. *Journal of Magnetism and Magnetic Materials*. 2010;322(18):2690-2695.
9. Akta S, Richardson GJ, Sellars CM. Hot Deformation and Recrystallization of 3% Silicon Steel Part 4: Effect of Recovery and Partial Recrystallization between Passes on Subsequent Recrystallization Behavior. *ISIJ International*. 2005;45(11):1696-1702.
10. Shimizu Y, Ito Y, Iida Y. Formation of the Goss orientation near the surface of 3 pct silicon steel during hot rolling. *Metallurgical Transactions A*. 1986;17(8):1323-1334.
11. Rajmohan N, Hayakawa Y, Szpunar JA, Root JH. Neutron diffraction method for stored energy measurement in interstitial free steel. *Acta Materialia*. 1997;45(6):2485-2494.
12. Park JT, Szpunar JA. Evolution of recrystallization texture in nonoriented electrical steels. *Acta Materialia*. 2003;51(11):3037-3051.
13. Liu JL, Sha YH, Zhang F, Yang HP, Zuo L. Development of strong {001} <210> texture and magnetic properties in Fe-6.5wt.%Si thin sheet produced by rolling method. *Journal of Applied Physics*. 2011;109(7):07A326.
14. Hölscher M, Raabe D, Lücke K. Rolling and recrystallization textures of bcc steels. *Materials Technology*. 1991;62(12):567-575.
15. Park JY, Han KS, Woo JS, Chang SK, Rajmohan N, Szpunar JA. Influence of primary annealing condition on texture development in grain oriented electrical steels. *Acta Materialia*. 2002;50(7):1825-1834.
16. Lu X, Xu YB, Fang F, Zhang YX, Wang Y, Jiao HT, et al. Microstructure, texture and precipitate of grain-oriented 4.5 wt% Si steel by strip casting. *Journal of Magnetism and Magnetic Materials*. 2016;404:230-237.
17. Zhang N, Yang P, Mao WM. Through process texture evolution of new thin-gauge non-oriented electrical steels with high permeability. *Journal of Magnetism and Magnetic Materials*. 2016;397:125-131.
18. Rouag N, Vigna G, Penelle R. Evolution of local texture and grain boundary characteristics during secondary recrystallisation of Fe-3% Si sheets. *Acta Metallurgica et Materialia*. 1990;38(6):1101-1107.
19. Harase J, Shimizu R. Influence of cold rolling reduction on the grain boundary character distribution and secondary recrystallization in nitrided Fe 3% Si alloy. *Journal of Magnetism and Magnetic Materials*. 2000;215-216:89-91.
20. Takahashi N, Suga Y, Kobayashi H. Recent developments in grain-oriented silicon-steel. *Journal of Magnetism and Magnetic Materials*. 1996;160:98-101.
21. Quadir MZ, Duggan BJ. A microstructural study of the origins of γ recrystallization textures in 75% warm rolled IF steel. *Acta Materialia*. 2006;54(16):4337-4350.
22. Haratani T, Hutchinson WB, Dillamore IL, Bate P. Contribution of shear banding to origin of Goss texture in silicon iron. *Metal Science*. 1984;18(2):57-66.
23. Mahesh S. Deformation banding and shear banding in single crystals. *Acta Materialia*. 2006;54(17):4565-4574.